Calcium-Binding Sites of Calmodulin and Electron Transfer by Inducible Nitric Oxide Synthase†

Irena Gribovskaja,‡ Kaleb C. Brownlow,‡ Sam J. Dennis,‡ Andrew J. Rosko,‡ Michael A. Marletta,§ and Regina Stevens-Truss*,‡

Department of Chemistry, Kalamazoo College, Kalamazoo, Michigan 49006, and Department of Chemistry, University of California, Berkeley, California 94720

Received December 6, 2004; Revised Manuscript Received March 4, 2005

ABSTRACT: Like that of the neuronal nitric oxide synthase (nNOS), the binding of Ca^{2+}-bound calmodulin (CaM) also regulates the activity of the inducible isoform (iNOS). However, the role of each of the four Ca^{2+}-binding sites of CaM in the activity of iNOS is unclear. Using a series of single-point mutants of *Drosophila melanogaster* CaM, the effect that mutating each of the Ca^{2+}-binding sites plays in the transfer of electrons within iNOS has been examined. The same Glu (E) to Gln (Q) mutant series of CaM used previously [Stevens-Truss, R., Beckingham, K., and Marletta, M. A. (1997) *Biochemistry 36*, 12337−12345] to study the role of the Ca^{2+}-binding sites in the activity of nNOS was used for these studies. We demonstrate here that activity of iNOS is dependent on Ca^{2+} being bound to sites II (B2Q) and III (B3Q) of CaM. Nitric oxide (•NO) producing activity (as measured using the hemoglobin assay) of iNOS bound to the B2Q and B3Q CaMs was found to be 41 and 43% of the wild-type activity, respectively. The site I (B1Q) and site IV (B4Q) CaM mutants only minimally affected •NO production (95 and 90% of wild-type activity, respectively). These results suggest that NOS isoforms, although all possessing a prototypical CaM binding sequence and requiring CaM for activity, interact with CaM differently. Moreover, iNOS activation by CaM, like nNOS, is not dependent on Ca^{2+} being bound to all four Ca^{2+}-binding sites, but has specific and distinct requirements. This novel information, in addition to helping us understand NOS, should aid in our understanding of CaM target activation.

Nitric oxide synthase (NOS,[1] EC 1.14.13.39) continues to be of clinical importance because of the varied intracellular roles of nitric oxide (•NO). Besides its normal physiological functions, including neuronal cell−cell signaling and immune responsiveness, when its production is unregulated •NO has been shown to play a part in several pathological conditions such as stroke and Alzheimer's disease, and may be involved in potentiating certain cancers. This physiologically important messenger is produced in a variety of cells from L-arginine and O_2 by NOS. Three distinct isoforms of NOS exist: neuronal (nNOS), endothelial (eNOS), and inducible (iNOS) (*1*). Similarities among the NOS isoforms include the fact that they are all homodimers, with each monomer possessing an N-terminal heme domain and a C-terminal reductase domain (*2*−*5*). The heme domain binds an iron protoporphyrin IX ring (*6*−*8*), H_4B (*5*, *9*−*11*), and L-arginine, and is where catalysis takes place. The reductase domain binds 1 equiv each of FAD and FMN, and is the site of interaction of NADPH, the exogenous electron-donating molecule (*9*, *11*, *12*). Electron transfer within NOS is triggered by the binding of Ca^{2+}-bound calmodulin (Ca^{2+}/CaM) to an amino acid sequence located approximately midway between the two domains (*13*−*17*). Besides tissue localization, the NOS isoforms also possess other differences. Of principal interest is their interaction with the ubiquitous Ca^{2+}-binding protein CaM. The nNOS and eNOS enzymes bind Ca^{2+}/CaM reversibly in response to Ca^{2+} levels, while iNOS binds Ca^{2+}/CaM in a seemingly irreversible fashion (*1*, *18*, *19*). Despite a number of studies that have focused on the interactions of peptides corresponding to the NOS CaM-binding sequences (*13*−*15*, *20*), the molecular nature of the interactions is still poorly understood. In addition, it is unknown if the fully Ca^{2+}-bound structure of CaM shown in Figure 1 is needed for activation of the three NOS isoforms.

† We gratefully acknowledge the Mac Arthur Fund (Kalamazoo College, R.S.-T.), The Mellon Foundation (R.S.-T.), and the Howard Hughes Medical Institute (R.S.-T. and M.A.M.) for project funding. Also, the Kaufman Fund (Department of Chemistry, Kalamazoo College, K.C.B. and A.J.R.), Kalamazoo College Faculty Development (K.C.B. and S.J.D.), and the Howard Hughes Medical Institute (I.G.) for student support.

* To whom correspondence should be addressed: Kalamazoo College, 1200 Academy St., Kalamazoo, MI 49006. Phone: (269) 337-7330. Fax: (269) 337-7251. E-mail: rtruss@kzoo.edu.

‡ Kalamazoo College.

§ University of California.

[1] Abbreviations: NOS, nitric oxide synthase; nNOS, neuronal nitric oxide synthase; iNOS, inducible nitric oxide synthase; eNOS, endothelial nitric oxide synthase; •NO, nitric oxide; CaM, calmodulin; H_4B, (6*R*)-5,6,7,8-tetrahydro-L-biopterin; Hepes, 4-(2-hydroxyethyl)piperazineethanesulfonic acid; BSA, bovine serum albumin; DTT, dithiothreitol; CAP, chloramphenicol; AMP, ampicillin; TB, Terrific broth; LB, Lauria−Bertani broth; IPTG, isopropyl β-D-thiogalactopyranoside; EGTA, ethylene glycol bis(β-aminoethyl ether)-*N*,*N*,*N*′,*N*′-tetraacetic acid; SDS−PAGE, sodium dodecyl sulfate−polyacrylamide gel electrophoresis; β-ME, β-mercaptoethanol; ECL, enhanced chemiluminescence; ICP, inductively coupled plasma atomic emission spectroscopy. In the mutant CaM nomenclature, B*x* denotes the Ca^{2+}-binding site while Q denotes the substituted residue (glutamine).

10.1021/bi0474517 CCC: $30.25
Published on Web 04/26/2005

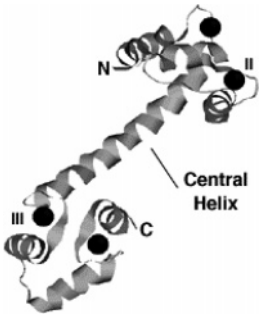

FIGURE 1: Ribbon diagrams depicting the fold of Ca^{2+}-bound CaM. Coordinates for this structure were taken from Brookhaven Protein Data Bank entry 1c11 (Ca^{2+}-bound CaM). In this NMR structure, the N- and C-termini are clearly indicated. Black spheres represent Ca^{2+} ions bound to each of the Ca^{2+}-binding sites. Sites II and III are indicated.

We have previously demonstrated that iNOS's tight interaction with CaM can be reversed (*21*). However, initial studies using EGTA to chelate Ca^{2+} suggested that the iNOS−CaM interaction was only partially reversible as only 30% of iNOS activity was inhibited (*21*). A synthetic peptide corresponding to the CaM-binding sequence from iNOS, however, was able to fully inhibit iNOS activity, and the inhibition was demonstrated to be the result of removal of the tightly bound CaM (*21*). That study demonstrated that like that of nNOS and eNOS, activity of iNOS requires its bound CaM as the peptide-induced inhibition was fully reversible with the addition of exogenous CaM. Furthermore, that study demonstrated the importance of Ca^{2+} in the interaction of CaM and iNOS, as the observed EGTA inhibition was reversed by the addition of Ca^{2+}. Whether iNOS's interaction with CaM and its subsequent activation require that Ca^{2+} be bound to one or all four Ca^{2+}-binding sites of CaM, until this report, has been a mystery. In fact, the role of the Ca^{2+}-binding sites of CaM in the interaction of CaM with any of the NOS isoforms is yet not understood.

In the case of nNOS, we have demonstrated that Ca^{2+}-binding site I of CaM is crucial for electron transfer within this isoform (*22*). On the other hand, nNOS is less dependent on Ca^{2+} being bound to site III of CaM. These results (i) showed that nNOS's activation by CaM does not require that Ca^{2+} be bound to all four sites, (ii) suggested that the antiparallel orientation previously demonstrated for CaM interacting with the CaM-binding sequence of nNOS may also exist in the intact protein, and (iii) demonstrated that additional interactions exist between CaM and nNOS outside of the putative CaM-binding domain that are critical to nNOS's activation. In that study, a series of mutant CaMs from *Drosophila* were used to assess the role of the Ca^{2+}-binding sites in the activity of nNOS. These mutant CaMs had previously been used to demonstrate the importance of the Ca^{2+}-binding sites in the activation of several CaM-binding proteins, as Ca^{2+} binding is important for target activation (*23*, *24*). Our results with these mutants as well as previous findings demonstrate that target activation involves specific Ca^{2+}-dependent interactions that are distinct from interactions required for protein−protein association. These results have led us to hypothesize that eNOS and iNOS also possess Ca^{2+}-dependent interactions that are specifically needed for enzyme activation. Studies to ascertain the specifics of eNOS activation by CaM are complicated by the fact that eNOS is membrane-bound, and is involved in regulation by several cell signaling mechanisms (*25*). Nonetheless, several studies have indicated that eNOS also possesses contacts with CaM that are responsible for its activity that are different from contacts solely involved in binding (*20*, *26*−*28*).

We report here that activation of iNOS, like that of nNOS, does not require that Ca^{2+} be bound to all four Ca^{2+}-binding sites of CaM. Moreover, as previously found for nNOS, activation of iNOS by CaM also involves specific Ca^{2+}-dependent interactions; however, the interactions appear to be different. Conclusions regarding the regions of CaM believed to be responsible for activation of iNOS will be made, and a structural representation of the CaM-bound iNOS will be proposed.

EXPERIMENTAL PROCEDURES

Materials and General Methods

Escherichia coli JM109 and BL21(DE3) competent cells and the pACYC184 plasmid vector were obtained from Novagen. All restriction enzymes were from Gibco BRL. QIAquick gel extraction and QIAfilter plasmid DNA purification kits were from Qiagen. Tryptone and yeast extract were from Difco. H_4B was purchased from Cayman Chemicals and prepared in 100 mM Hepes (pH 7.4) containing 100 mM dithiothreitol (DTT). 2′,5′-ADP Sepharose 4B, Superdex 200 prep grade, ECL reagents, and Hi-Trap Desalting columns were from Amersham-Pharmacia LKB Biotechnology, Inc. Bradford protein dye reagent, Chelex 100 resin, and all electrophoresis reagents were from Bio-Rad. Ultrafree-15 centrifugal filtration units were from Millipore. All other reagents, unless otherwise stated, were from Sigma Chemical.

Subcloning of Drosophila CaMs

The genes for *Drosophila* wild-type and mutant CaMs (E to Q mutant series) were subcloned into the pACYC184 vector from a pEMBL8 vector (generous gift of K. Beckingham, Rice University, Houston, TX) using HindIII and SalI restriction sites (*29*). Digested segments were separated on 1% agarose gels, and the bands of interests were cut out of the gel and purified using DNA QIAquick gel extraction kit following the manufacturer's procedures. The purified fragments corresponding to the CaM genes were each then ligated using T4 DNA ligase into the pACYC184 vector previously digested with HindIII and SalI. The CaM genes were introduced into the pACYC184 vector in the tetracycline resistance gene location on the plasmid (see New England BioLabs DNA sequence map at www.neb.com). Chloramphenicol (CAP) resistance was retained in the new pACYC-CaM vectors, allowing for CAP resistance selection capabilities. The integrity of the digested DNA and proper CaM sequence insertion into the pACYC184 vector was assessed using AvaI, EcoRI, and XbaI, in separate restriction enzyme combination experiments, monitored on 1% agarose gels. The pACYC-CaM plasmids were then amplified in *E. coli* JM109 cells, and purified using QIAfilter DNA plasmid kits following the manufacturer's protocols.

iNOS Expression

To obtain active, holo-iNOS, its coexpression with calmodulin is necessary, as previously demonstrated (*30*, *31*). *E.*

coli BL21(DE3) cells were transformed with the plasmids for both iNOS (pCW-iNOS) and CaM (pACYC-CaM) as previously described (*32*). Separate transformation experiments were carried out for each *Drosophila* CaM that was studied. BL21(DE3) double transformants were selected using LB agar containing AMP (100 μg/mL) and CAP (64 μg/mL), grown for 16−20 h at 37 °C. Freshly transformed cells (single colonies) were then transferred to a 60 mL TB starter liquid culture containing AMP (100 μg/mL) and CAP (64 μg/mL), and grown for 12−18 h at 37 °C. An aliquot of the starter culture (10 mL) was transferred to 750 mL of TB medium (also containing AMP and CAP) and allowed to grow at 37 °C until the OD_{600} reached ∼0.4. The incubator temperature was reduced to 24 °C, and the cells were grown for an additional 1 h or until the OD_{600} reached ∼0.6. IPTG (0.4 mM) was then added to the cultures to induce protein expression, and these were maintained at 24 °C for 36−42 h. Cells were then harvested by centrifugation, resuspended in sonication buffer [50 mM Hepes (pH 7.4), 20% glycerol, 10−15 μM H_4B, and protease inhibitors], and stored at −70 °C until further use.

Purification of the iNOS−CaM Complex

As the interaction of iNOS and CaM is strong and seemingly independent of intracellular levels of calcium, iNOS and CaM presumably interact immediately following expression. iNOS was expressed with each *Drosophila* CaM (wild type or each calcium-binding site mutant) as described above. Purification was achieved following previously reported protocols (*11*, *33*) with modifications. Cells previously frozen in sonication buffer were thawed on ice and lysed by sonication (5 × 30 s, at a setting of 4 using a Sonic Dismembrator, Fisher). The cell homogenate was then centrifuged at 37000*g* to separate the soluble (supernatant) from the insoluble fractions. Supernatant (30 000 units of activity measured using the hemoglobin assay described below) was then applied to a 2′,5′-ADP Sepharose 4B column (5 g) previously equilibrated with buffer A [50 mM Hepes, 10% glycerol, and 0.5 mM L-arginine (pH 7.4)]. The protein-loaded column was then washed sequentially with buffer A (30 mL), buffer B (buffer A with 2 mM adenosine 5′-diphosphate, 5′-ADP, and 0.5 M NaCl, 60 mL), and buffer C [50 mM Hepes and 10% glycerol (pH 7.4), 30 mL], and the protein was eluted with buffer D (buffer C with 1.0 mM $NADP^+$ and 3.0 mM NADPH, 50 mL) directly into an UltraFree-15 centrifugal concentrator and concentrated to ∼1 mL. The concentrator contents were then washed with 10 mL of buffer C and reconcentrated to ∼1 mL. All column washes and concentrator buffer changes contained 10−15 μM H_4B. Concentrated protein samples were applied to a Superdex 200 (S200) column (47.5 cm × 1.0 cm) previously equilibrated with buffer C containing 10−15 μM H_4B and 100 mM βME. This column was run under low pressure until all the protein was eluted. Fractions that were found to contain NOS protein bound to high-spin heme (determined spectrophotometrically as a peak centered at ∼400 nm and possessing a heme-to-flavin ratio of ≥3) were pooled, concentrated in an UltraFree-15 centrifugal concentrator, and stored at −70 °C in the presence of 20% glycerol and 10−15 μM H_4B. The purification efficiency and purity of the various iNOS−CaM complexes were assessed by SDS−PAGE. Protein concentrations were determined by Bradford analysis.

SDS−PAGE and Western Analyses

iNOS expression was analyzed on 12% acrylamide gels under denaturing conditions. *E. coli* cells were suspended in sonication buffer and frozen at −70 °C for a minimum of 24 h. Before analysis, samples were sonicated, and cell lysates (10 μg of total protein per lane) were loaded into separate lanes of the gels and electrophoresed at a constant voltage (180 V) for 70−90 min. Following electrophoresis, proteins were transferred to a nitrocellulose membrane. The membranes were then probed with rabbit-grown polyclonal antibodies against iNOS, followed by treatment with horseradish peroxidase-conjugated anti-rabbit IgG antibodies. iNOS detection was achieved using ECL reagents.

iNOS purification was monitored by SDS−PAGE on 12% acrylamide gels. Aliquots of protein samples from each step in the purification were obtained and treated with SDS−PAGE sample buffer. To each lane was added 3−8 μg of protein, and samples were electrophoresed at a constant voltage (180 V) for 70−90 min. Protein was visualized by staining with Coomasie Blue.

Determination of Metal (calcium, iron, and zinc) Content

To assess the number of calcium ions bound to calmodulin in the iNOS−CaM complex, as well as to determine the iron and zinc content of iNOS, the method of ICP analysis was used. Metal-free samples were obtained as previously described (*33*) with the following modifications. Purified iNOS−CaM proteins were desalted using a Hi-Trap desalting column (Amersham-Pharmacia) that had been equilibrated with metal-free 20 mM Hepes (pH 7.4). Metal-free buffer was obtained by slowly passing the solution through a Chelex-100 column (32.5 cm × 2.5 cm) and collecting the eluent directly into a previously acid-washed container. Using a 30 mL syringe, chelated 20 mM Hepes (pH 7.4, 20 mL) was run through a 5 mL Hi-Trap desalting column to equilibrate the beads. Using a 1 mL syringe, the purified iNOS−CaM protein was added to the equilibrated Hi-Trap column, and the protein was eluted by passing chelated buffer through the column using a 30 mL syringe. Aliquots (0.5 mL) were collected directly into 1.7 mL microcentrifuge tubes. Protein concentrations were determined by Bradford analysis, and the samples were analyzed for metal content by ICP analysis (Department of Geological Sciences, University of Michigan, Ann Arbor, MI).

Spectral Characterization of the iNOS−CaM Complex

Spectra were obtained on a Cary 3E spectrophotometer equipped with a circulating water bath set at 10 °C. Purified samples (400 μL, 1.0−4.0 μM) in 50 mM Hepes (pH 7.4) containing glycerol (10%) were placed in a quartz cuvette, and spectra were recorded.

Arginine Binding. Concentrations of L-arginine from 0 to 500 μM were added to a cuvette containing protein, and spectra were recorded after each addition. The change in absorbance at 381 nm was subtracted from the change at 418 nm ($\Delta\Delta$ absorbance 381−418) for each spectrum recorded, and these differences were plotted against L-

arginine concentration. Binding constants (K_d) were determined by nonlinear regression using KaleidaGraph (Reading, PA).

Formation of the Ferrous−CO Complex. Following each arginine binding experiment (final L-arginine binding spectra), excess dithionite was added to the cuvette containing iNOS, and spectra were recorded. CO gas was then gently added directly to the solution in the cuvette followed by its addition directly to the headspace for 5−10 min on ice, and spectra again were recorded.

Activity Assays

The electron transfer ability of iNOS in the presence of the various *Drosophila* CaMs was assessed either by the formation of methemoglobin or by monitoring cytochrome *c* reduction.

Hemoglobin assays were carried out as previously described (*34*) with the following modifications. iNOS bound to each of the *Drosophila* CaMs (5−10 nM) was incubated with L-arginine (1 mM), H_4B (10−20 μM), DTT (200−400 μM), glycerol (10%), oxyhemoglobin (7−10 μM), and Hepes (50 mM, pH 7.4). Assays (1 mL) were initiated with NADPH (240 μM), and were monitored at 401 nm and 37 °C. Activities were determined using an extinction coefficient of 60 000 M^{-1} cm^{-1} for the increase in absorbance at 401 nm, indicative of the production of methemoglobin. Assays carried out for the determination of L-arginine K_m values were conducted by varying the concentration of L-arginine from 1 to 1000 μM. Specific activities were then plotted against L-arginine concentrations, and K_m values were determined by nonlinear regression using KaleidaGraph.

Cytochrome c assays were carried out as previously described (*5*, *22*) with the following modifications. iNOS bound to each of the *Drosophila* CaMs (4−7 nM) was assayed in Hepes (50 mM, pH 7.4), glycerol (10%), and cytochrome *c* (50 μM). Assays (1 mL) were initiated with NADPH (240 μM), and were monitored at 550 nm and 37 °C. Activities were determined using a change in extinction coefficient of 21 000 M^{-1} cm^{-1}.

Statistical Analyses

Comparisons of the means were made using a Student's *t* test, with the values assessed at the 95% confidence interval.

RESULTS

Expression and Purification of CaM-Bound, Active, Intact Holo-iNOS. Active inducible NOS is typically isolated from cells tightly bound to CaM. For this reason, expression of active, soluble iNOS was only afforded upon its coexpression with the various *Drosophila* CaMs. *E. coli* cells transformed with both the iNOS plasmid (pCW-iNOS) and any of the CaM plasmids (pACYC-CaM) were found to express intact, soluble iNOS at high levels. SDS−PAGE followed by Western analysis demonstrated that iNOS expressed in cells up to 24 h post-IPTG induction was rapidly proteolyzed intracellularly (Figure 2). High levels of peptides that migrated at molecular masses that corresponded to the heme and reductase domain of iNOS that also reacted with iNOS polyclonal antibodies were detected by Western analysis (Figure 2). When cells were allowed to express protein for 36−42 h post-induction, high levels of intact, active iNOS

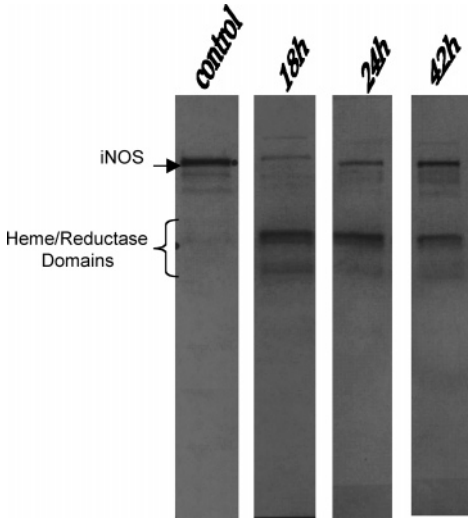

FIGURE 2: Western analysis of post-induction time-dependent iNOS expression. *E. coli* cell lysate samples were run on SDS−PAGE gels (12%), and then proteins were transferred to a nitrocellulose membrane. Membranes were probed with polyclonal antibodies to iNOS, and proteins were visualized by chemiluminescence. The iNOS control lane corresponds to a purified iNOS control sample. The heme/reductase domain bands were determined by comparison to purified samples run in separate lanes on the same gels. The time labels for each lane correspond to the time of protein expression in the cells post-IPTG induction.

were obtained (Figure 2). Purification was achieved using a combination of two columns. First, the 2′,5′-ADP column separated the iNOS−CaM complex from other *E. coli* proteins, as these were washed off with the first buffer wash (Figure 3A, lanes 2 and 3). Loosely bound impurity proteins were removed by washing the column with a buffer containing 5′-ADP. As can be seen in Figure 3A (lane 4), several protein bands were lost from the sample after the 5′-ADP wash with a minimal loss of NOS protein. Protein obtained from this step was deemed to be <50% pure (Figure 3A, lane 6). In reported protocols (*11*, *32*), a DEAE-Bio-Gel A ion exchange column is typically used as the second step in NOS purification. However, this resin proved to be ineffective in our procedures as very few impurities were removed (data not shown). Size exclusion chromatography using a Superdex-200 (S200) gel filtration column afforded proteins that were deemed >95% pure (Figure 3A, lane 10, and Figure 3B), assessed from the FlurS-scanned images quantified using QuantOne (Bio-Rad). S200 fractions loaded into lanes 7 and 8 (Figure 3A), although appearing to correspond to the pure iNOS protein, were found to contain low-spin heme iNOS as determined spectrophotometrically; λ_{max} values of iNOS were broad and slightly red shifted (data not shown).

Characterization of E. coli-Expressed iNOS Bound to Various Drosophila CaMs. All of the purified recombinant iNOSs bound to *Drosophila* CaMs possess spectral and L-arginine binding properties identical to those of iNOS bound to human CaM (*32*). They were all found to be purified bound to a high-spin heme with a λ_{max} centered at ~400 nm as shown in the representative spectrum in Figure 4. In all cases, the iNOS−CaM complex bound L-arginine and demonstrated the typical blue shift representative of substrate binding (Figure 4A). Arginine binding constants (K_d) were spectrally found to be between 6 and 13 μM (Table 1), in agreement with published values (*32*). Arginine K_m

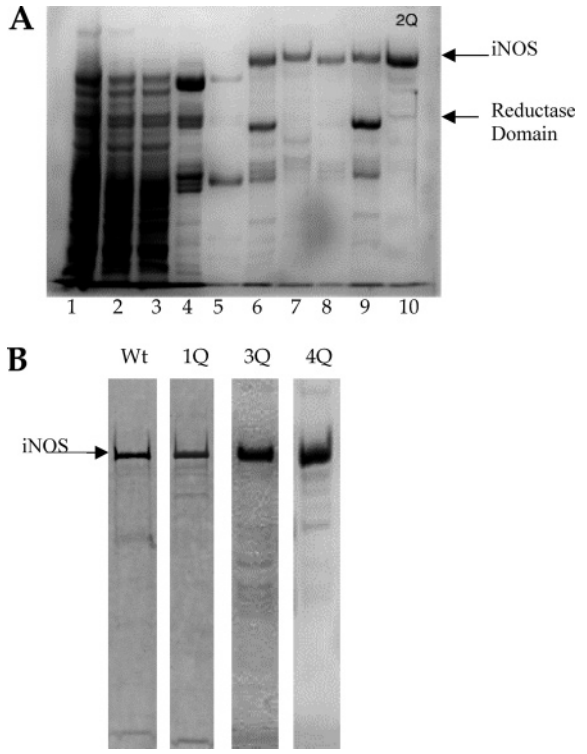

FIGURE 3: SDS−PAGE analysis of the purification of recombinant iNOS bound to *Drosophila* CaMs. Aliquots from each step in the purification protocol were treated with SDS sample buffer and loaded into separate wells of 12% acrylamide gels. Electrophoresis was carried out under denaturing conditions, and proteins were visualized using Coomassie Blue. Panel A is a representative gel showing samples from the fractions from both columns in the purification. The protein in lane 10 is an aliquot of the purified, concentrated, iNOS−B2Q-CaM (2Q) enzyme: lane 1, supernatant loaded onto column 1 (ADP-Sepharose); lane 2, column 1 flowthrough; lane 3, column 1 buffer A wash; lane 4, column 1 buffer B wash; lane 5, column 1 buffer C wash; lane 6, column 1 eluent; lane 7, fraction from column 2 (S200 Superdex) spectrally determined to contain low-spin heme iNOS; lane 8, fraction from column 2 that contained spectrally sound, pure iNOS; and lane 9, fraction from column 2 that contained a principally reductase contaminant, as determined spectrally. Panel B shows the lanes from representative gels that corresponded with lane 10 in panel A but that were obtained for iNOS purified bound to wild-type (Wt), site I mutant (1Q), site III mutant (3Q), and site IV mutant (4Q) CaMs.

values were also determined for iNOS bound to each *Drosophila* CaM (wild type and mutant) using the hemoglobin assay. Values of K_m were found to be between 7 and 15 μM (Table 1), in the range of published values for murine macrophage iNOS (*11*). All of the recombinant iNOS proteins were also found to form the prototypical P450 spectrum in response to the iron being reduced in the presence of CO (Figure 4B). These parameters demonstrated that *E. coli* indeed expressed an iNOS protein that was similar to iNOS isolated from other sources.

Given that the CaM proteins used in this study were mutated at one of the Ca^{2+}-binding sites, it was crucial to determine the amount of Ca^{2+} bound to each of these recombinant iNOS proteins. Additionally, assessment of the amount of metals bound to iNOS is important for characterization of enzymatic activity. Metal analysis done by the method of ICP demonstrated that regardless of the *Drosophila* CaM protein bound to iNOS, all recombinant proteins purified with approximately one iron (0.8−1.5 per iNOS monomer) and one zinc (0.7−0.9 per iNOS monomer) (Table 2). When bound to wild-type CaM, iNOS proteins were found to bind four calcium ions per monomer. However, when bound to any of the four mutated CaMs, iNOS was found to possess only three calcium ions per molecule, as expected (Table 2).

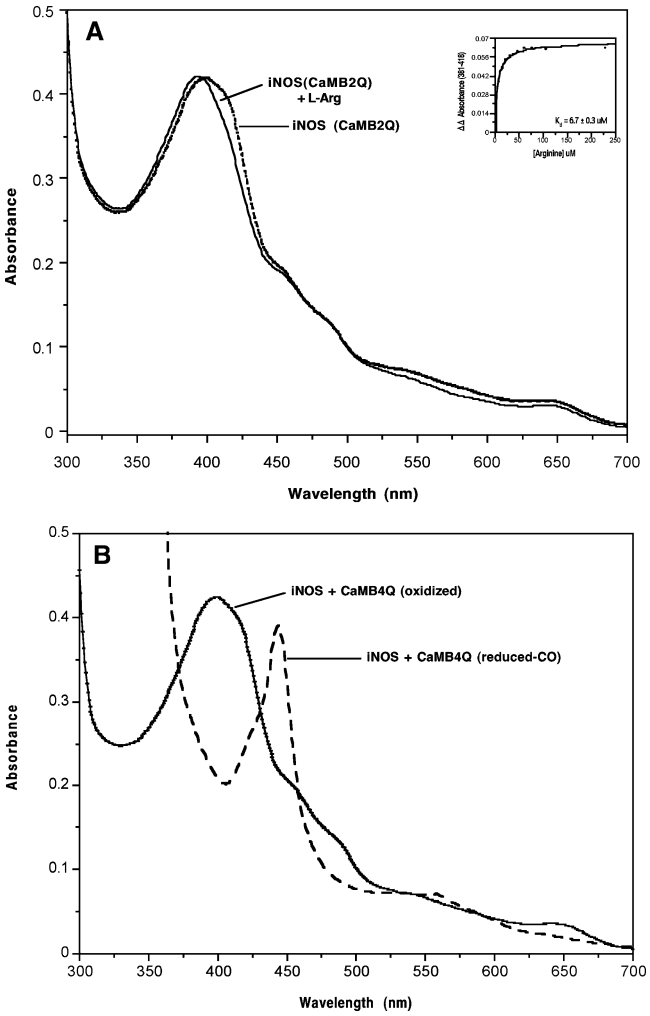

FIGURE 4: Spectral analysis of recombinant iNOS in the presence of mutated *Drosophila* CaMs. All spectral analyses were carried out on a Cary 300 spectrophotometer equipped with a circulating water bath set at 10 °C. (A) To the purified iNOS−B2Q-CaM complex (4.0 μM) was added arginine, incrementally, from 0 to 500 μM, and spectra were recorded after each addition. The solid spectrum is that of iNOS in the absence of arginine (λ_{max} centered at ∼400 nm). The dotted spectrum is that of iNOS bound to arginine (500 μM, λ_{max} observed to shift to ∼393 nm). (B) To the purified iNOS−B4Q-CaM complex (4.1 μM) was first added arginine to generate the arginine binding spectrum (not shown in panel B), and then the iron was reduced with dithionite followed by the addition of carbon monoxide (CO) to the sample. The solid spectrum is that of oxidized iNOS in the absence of arginine (λ_{max} centered at ∼400 nm). The dotted spectrum is that of reduced iNOS bound to arginine (500 μM) and CO (λ_{max} centered at ∼444 nm).

Effect that CaM Mutations Have on iNOS Activities. The ability of iNOS to transfer electrons was analyzed in two ways. First, iNOS proteins were assayed for their ability to reduce cytochrome *c*, which is a measure of the extent of electron transfer within the reductase domain. The results show that maximal cytochrome *c* reduction (∼20 μmol min^{-1} mg^{-1}) was observed for iNOS bound to either the wild type or the site I mutant (B1Q) of CaM (Table 3). When bound to the B2Q and B3Q mutant CaMs, iNOS was found to reduce cytochrome *c* by only 65 and 68% of the wild-type

Table 1: Arginine Binding Constants for Recombinant iNOS in the Presence of *Drosophila* CaMs

calmodulin	K_d (μM)[a]	K_m (μM)[b]
wild-type	13.08 ± 0.58	7.80 ± 1.56
B1Q	8.47[c] ± 1.36	9.71 ± 1.88
B2Q	6.70[c] ± 0.31	10.80 ± 1.70
B3Q	10.16 ± 0.79	14.20[c] ± 1.29
B4Q	12.40 ± 1.20	14.50[c] ± 4.10

[a] Values were determined spectrophotometrically as described in Experimental Procedures. [b] Values were determined using the hemoglobin assays as described in Experimental Procedures. The values represent the average of two or more experiments ± the standard error of the mean. [c] This value is statistically different from the corresponding wild-type values when $p = 0.05$.

Table 2: Metal Content of Recombinant iNOS in the Presence of *Drosophila* CaMs[a]

	no. of metals per iNOS molecule[b]		
calmodulin	calcium	iron	zinc
wild-type	3.98 ± 0.07	0.81 ± 0.11	0.75 ± 0.09
B1Q	2.81[c] ± 0.21	0.82 ± 0.08	0.68 ± 0.11
B2Q	3.08[c] ± 0.20	1.50 ± 0.20	0.82 ± 0.13
B3Q	3.12[c] ± 0.17	1.39 ± 0.30	0.80 ± 0.16
B4Q	3.26[c] ± 0.30	1.60[c] ± 0.12	0.87 ± 0.08

[a] All analyses of metal content were carried out by the method of ICP at the University of Michigan. [b] Values represent the molar ratio of metal to iNOS protein molecule. Errors are the standard error of the means based on two or more analyses per sample. [c] This value is statistically different from the corresponding wild-type values when $p = 0.05$.

Table 3: Activity of Recombinant iNOS Bound to Various *Drosophila* CaMs[a]

	specific activity[b]	
calmodulin	cytochrome *c* reduction (μmol min^{-1} mg^{-1})[c]	methemoglobin formation (nmol min^{-1} mg^{-1})[d]
wild-type	20.1 ± 1.2	936.6 ± 42.5
B1Q	21.9 ± 3.3	893.9 ± 3.4
B2Q	12.9 ± 1.1	386.5 ± 23.8
B3Q	13.6 ± 1.8	399.8 ± 12.8
B4Q	8.6 ± 0.7	842.4 ± 3.5

[a] The values were calculated from three or more experiments performed in duplicate. Errors are the standard error of the mean. [b] Values are the maximal velocities observed for iNOS in the presence of the given CaM mutant. The amount of protein was determined by Bradford analysis. [c] Assays contained iNOS (4−7 nM) and cytochrome *c* (50 M), and were monitored at 550 nm as described in Experimental Procedures. [d] Assays contained iNOS (5−10 nM) and hemoglobin (7−10 μM), and were monitored at 401 nm as described in Experimental Procedures.

level, respectively, and in the presence of the site IV mutant CaM (B4Q), the level of cytochrome *c* reduction was found to be 43% of that of the wild type (Table 3). These results suggest that electron transfer by the reductase domain of iNOS requires that CaM have Ca^{2+} at sites II−IV. Second, the ability of iNOS to produce •NO when bound to each CaM mutant was assessed by monitoring formation of methemoglobin. Nitric oxide is produced by NOSs as a result of the heme iron being reduced by electrons donated by FMN in the reductase domain (*35*). By monitoring methemoglobin formation, therefore, we assessed the transfer of electrons through the reductase and heme domains of iNOS. The •NO forming activity of iNOS bound to wild-type *Drosophila* CaM was found to be 0.89−1.0 μmol min^{-1} mg^{-1}. This value is in agreement with the previously published values for iNOS (*32*). As shown in Table 3, mutation of Ca^{2+}-binding site I or IV of CaM had little effect on the •NO forming activity of iNOS (95% of wild-type CaM activity observed with the B1Q mutant and 90% with the B4Q mutant). Ca^{2+} bound to sites II (B2Q) and III (B3Q) of CaM, however, appears to be crucial to electron transfer within iNOS. Only 41 and 43% of wild-type CaM •NO producing activity was found for iNOS bound to the B2Q and B3Q mutants, respectively (Table 3). It appears then that activation of iNOS by CaM requires that Ca^{2+}-binding sites II and III have Ca^{2+} bound to them. Ca^{2+}-binding site IV of CaM appears to be primarily involved in electron transfer by the iNOS reductase domain to exogenous acceptors, such as cytochrome *c*.

DISCUSSION

For a number of years, we have been interested in the regulation of NOS activity by CaM. All NOS isoforms isolated to date are CaM-activated proteins (*36*). Calmodulin interactions, however, are believed to be different and unique between the NOS isoforms. The CaM-binding domains of the three NOS isoforms exhibit little sequence homology, with the two constitutive forms (nNOS and eNOS) having more homology between them than between them and iNOS (*36*). The interactions of the various NOSs with CaM have also been used to divide NOS into forms that bind CaM reversibly (nNOS and eNOS, dependent on Ca^{2+} concentrations) and those that interact in an irreversible fashion (namely, iNOS, which is irresponsive to Ca^{2+} concentrations). Although all three NOS isoforms have been shown to possess a prototypical CaM-binding sequence (*2*, *37*, *38*), additional contacts peripheral to that sequence are believed to exist. Our data suggest that these contacts are distinct between the NOS isoforms, and they therefore represent potential drug target sites.

The neuronal isoform of NOS has been shown to interact with CaM in an antiparallel orientation. This was observed by crystallographic analysis of CaM bound to the putative nNOS CaM-binding peptide, and the structure indicates that the interaction of these two proteins is prototypical of Ca^{2+}-dependent CaM-binding proteins such as MLCK (*15*). Previously published biochemical data further support that, and additionally demonstrate that Ca^{2+}-binding site I of CaM is crucial to electron transfer by nNOS (*22*). Furthermore, those results suggest that CaM's Ca^{2+}-binding site I exerts its action via the reductase domain of nNOS.

The study presented here was conducted in an effort to determine what role each of the Ca^{2+}-binding sites of CaM plays in the activity of iNOS. The results obtained demonstrate that wild-type *Drosophila* CaM is able to fully activate iNOS, as observed with nNOS. However, activation of these two NOS isoforms appears to occur by different mechanisms, as the *Drosophila* CaM mutants had a differential effect on their activities. In the presence of wild-type *Drosophila* CaM, iNOS was found to produce •NO and reduce cytochrome *c* at rates that were similar to reported values (*31*, *32*, *39*). When iNOS was isolated bound to the site IV mutant CaM (B4Q), however, a surprising and unexpected result was obtained. While the B4Q CaM significantly affected intra- and intermolecular electron transfer by nNOS (*22*), it only affected intermolecular electron transfer by iNOS, as cyto-

chrome *c* reduction was significantly affected (43% of wild-type activity measured) while methemoglobin formation was not (90% of wild-type activity measured) (data presented in Table 3). Moreover, Ca^{2+} binding to site IV of CaM was found to affect nNOS's ability to produce methemoglobin to a greater extent (*22*). Another differentiating finding was that activities of iNOS bound to the site II (B2Q) or site III (B3Q) CaM mutant were indistinguishable from each other (Table 3). However, these mutant CaMs had very different effects on the activities of nNOS; the B2Q CaM affected both the intra- and intermolecular activity of nNOS, while the B3Q CaM had little effect on either activity (*22*).

Perhaps the most interesting results were obtained with the site I mutant CaM (B1Q). When bound to B1Q CaM, nNOS was unable to catalyze any activity (*22*). However, in the presence of the B1Q CaM, iNOS activities were observed to be identical to the corresponding activities measured with wild-type CaM (see Table 3). One hypothesis that could explain the observed activities of iNOS bound to the B1Q CaM could be that upon CaM binding to iNOS the site interacts with Ca^{2+}. However, metal analysis showed that when bound to iNOS none of the mutant CaMs regained their ability to bind Ca^{2+} at the mutated site (data listed in Table 2). Therefore, the effects observed with any of these mutant CaMs suggest that different contacts between CaM and these enzymes exist, and that these contacts play a crucial role in their activation.

To the best of our knowledge, this is the first investigation wherein the role of specific factors of the CaM structure in the activation of iNOS has been reported. Data obtained with these mutant CaMs conclusively show that activation of iNOS requires Ca^{2+}. We previously demonstrated the need for Ca^{2+} in the activity of iNOS using the EGTA, but this Ca^{2+} chelator only reduced iNOS activity by 30% (*21*). We hypothesized at that time that iNOS activation by CaM did not require Ca^{2+} binding to all four sites. The results presented here support that hypothesis since the •NO producing activity of iNOS is nearly maximal when site I or site IV of CaM is Ca^{2+}-free (data presented in Table 3).

The data obtained with this series of Ca^{2+}-binding site mutant CaMs support the hypothesis that CaM differentially affects activation of the NOS isoforms. The biochemical data obtained in our previous study of nNOS's activation by these CaM mutants allowed for a proposed representation of the CaM-bound nNOS molecule (*22*). The results presented here for iNOS can also be used to hypothesize about a CaM-bound structure of iNOS. Figure 5 provides a simplification of our previously proposed nNOS structure (Figure 5A). We proposed here that iNOS interacts with CaM as represented in the schematic shown in Figure 5B. In as much as biochemical data can yield information regarding a protein's structure, our results using these *Drosophila* CaMs suggest that nNOS binds CaM in an antiparallel orientation and that iNOS may interact in a parallel orientation. Although CaM typically binds to its targets in an antiparallel orientation, the precedent for a parallel hypothesis comes from the demonstrated interactions of melittin with CaM (*40*−*42*). Moreover, the structure of CaM is believed to be highly flexible and promiscuous since CaM interacts with more than 30 different targets intracellularly (*43*), and it is thought that target peptide sequences determine the directionality of CaM

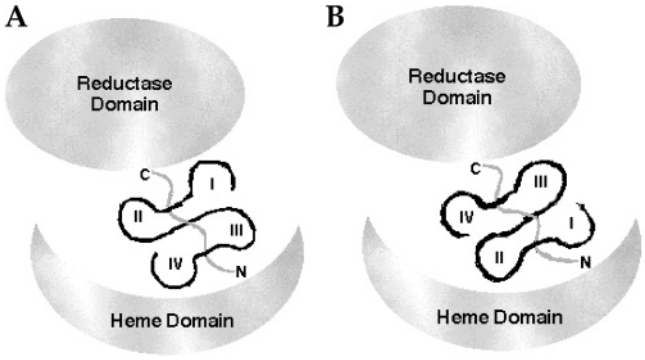

FIGURE 5: Schematic representations of potential structures of iNOS bound to CaM. Representations are based on our previously proposed structure of nNOS bound to CaM (*22*). In these schematics, the reductase and heme domains of NOS have been simplified so they do not detract from the main message. Their approximate location relative to one another, however, is the same as previously proposed. The NOS CaM-binding peptide sequence is represented by the squiggly line with the C-terminus and N-terminus labeled. The Roman numerals correspond to each of the Ca^{2+}-binding sites of CaM with the central helix given as the straight line that runs from the numeral II to III in each structure. Panel A is representative of the CaM-bound nNOS structure. The N-terminal lobe of CaM (possessing sites I and II) is shown to interact with the C-terminus of the nNOS CaM-binding peptide sequence, while the C-terminal lobe of CaM (possessing sites III and IV) interacts with the nNOS N-terminus. This is representative of an antiparallel orientation of these two proteins relative to one another. Panel B is representative of our currently proposed structure of iNOS bound to CaM. This schematic is being proposed on the basis of the biochemical data obtained in this study. The data suggest that iNOS binds CaM in a parallel orientation; therefore, the C-terminal lobe of CaM has been placed closer to the C-terminus of iNOS, and the N-terminal lobe is closer to the N-terminus.

(*44*). Directionality of CaM may be dictated by its binding to NOSs, and the overall topology of the quaternary structure of these proteins may provide another distinguishing feature of this family of enzymes.

The biochemical data presented here for iNOS bound to these CaM mutants suggest that crucial contacts exist between iNOS and regions of CaM that are exposed upon Ca^{2+} binding to specific sites of CaM. When these sites are Ca^{2+}-free, CaM may not adopt the required conformation to fully activate iNOS. Understanding how CaM binds to and activates its target proteins continues to be the subject of investigations. Guptaroy and colleagues have previously suggested that the pattern of target recognition by CaM involves specific Ca^{2+}-binding site interactions (*24*). The differential responses seen for iNOS and nNOS when bound to these mutants further support that notion. Investigations that will help in deciphering the molecular details of CaM's interaction with the NOSs that results in subsequent regulation of their functions are underway.

ACKNOWLEDGMENT

We thank Dr. Michelle Spiering for her help with the initial development of the overexpression system for iNOS. We also thank Dr. Kate Beckingham (Rice University) for providing the *Drosophila* CaM plasmids used to subclone the DNA into the pACYC184 vector. Our gratitude is also extended to Ms. Patrice Fields and Dr. Amy Hurshman for useful discussions of this project, to Mr. Ted Huston (University of Michigan) for his help and advice while

acquiring metal content data, and Dr. Tom Smith (Kalamazoo College) for his help with demineralization.

REFERENCES

1. Marletta, M. A. (1994) Nitric oxide synthase: Aspects concerning structure and catalysis, *Cell 78*, 927−930.
2. Bredt, D. S., Hwang, P. M., Glatt, C. E., Lowenstein, C., Reed, R. R., and Snyder, S. H. (1991) Cloned and expressed nitric oxide synthase structurally resembles cytochrome P-450 reductase, *Nature 351*, 714−718.
3. McMillan, K., and Masters, B. S. S. (1995) Prokaryotic Expression of the Heme- and Flavin-Binding Domains of Rat Neuronal Nitric Oxide Synthase as Distinct Polypeptides: Identification of the Heme-Binding Proximal Thiolate Ligand as Cysteine-415, *Biochemistry 34*, 3686−3693.
4. Richards, M. K., and Marletta, M. A. (1994) Characterization of Neuronal Nitric Oxide Synthase and a C415H Mutant, Purified from a Baculovirus Overexpression System, *Biochemistry 33*, 14723−14732.
5. Richards, M. K., Clague, M. J., and Marletta, M. A. (1996) Characterization of C415 Mutants of Neuronal Nitric Oxide Synthase, *Biochemistry 35*, 7772−7780.
6. McMillan, K., Bredt, D. S., Hirsch, D. J., Snyder, S. H., Clark, J. E., and Masters, B. S. S. (1992) Cloned, expressed rat cerebellar nitric oxide synthase contains stoichiometric amounts of heme, which binds carbon monoxide, *Proc. Natl. Acad. Sci. U.S.A. 89*, 11141−11145.
7. Stuehr, D. J., and Ikeda-Saito, M. (1992) Spectral Characterization of brain and macrophage nitric oxide synthases, *J. Biol. Chem. 267*, 20547−20550.
8. White, K. A., and Marletta, M. A. (1992) Nitric oxide synthase is a cytochrome P-450 type hemoprotein, *Biochemistry 31*, 6627−6631.
9. Mayer, B., John, M., Heinzel, B., Werner, E. R., Wachter, H., Schultz, G., and Böhme, E. (1991) Brain nitric oxide synthase is a biopterin- and flavin-containing multi-functional oxido-reductase, *FEBS Lett. 288*, 187−191.
10. Hevel, J. M., and Marletta, M. A. (1992) Macrophage nitric oxide synthase: Relationship between enzyme-bound tetrahydrobiopterin and synthase activity, *Biochemistry 31*, 7160−7165.
11. Hevel, J. M., White, K. A., and Marletta, M. A. (1991) Purification of the inducible murine macrophage nitric oxide synthase: Identification as a flavoprotein, *J. Biol. Chem. 266*, 22789−22791.
12. Stuehr, D. J., Cho, H. J., Kwon, N. S., Weise, M. F., and Nathan, C. F. (1991) Purification and characterization of the cytokine-induced macrophage nitric oxide synthase: An FAD- and FMN-containing flavoprotein, *Proc. Natl. Acad. Sci. U.S.A. 88*, 7773−7777.
13. Vorherr, T., Knopfel, L., Hofmann, F., Mollner, S., Pfeuffer, T., and Carafoli, E. (1993) The Calmodulin Binding Domain of Nitric Oxide Synthase and Adenylyl Cyclase, *Biochemistry 32*, 6081−6088.
14. Zhang, M., and Vogel, H. J. (1994) Characterization of the calmodulin-binding domain of rat cerebellar nitric oxide synthase, *J. Biol. Chem. 269*, 981−985.
15. Zhang, M., Yuan, T., Aramani, J. M., and Vogel, H. J. (1995) Interaction of Calmodulin with Its Binding Domain of Rat Cerebellar Nitric Oxide Synthase, *J. Biol. Chem. 270*, 20901−20907.
16. Abu-Soud, H. M., and Stuehr, D. J (1993) Nitric oxide synthases reveal a role for calmodulin in controlling electron transfer, *Proc. Natl. Acad. Sci. U.S.A. 90*, 10769−10772.
17. Abu-Soud, H. M., Yoho, L. L., and Stuehr, D. J. (1994) Calmodulin Controls Neuronal Nitric-oxide Synthase by a Dual Mechanism: Activation of intra- and inter-domain electron transfer, *J. Biol. Chem. 269*, 32047−32050.
18. Nathan, C. (1992) Nitric oxide as a secretory product of mammalian cells, *FASEB J. 6*, 3051−3064.
19. Cho, H. J., Xie, Q.-W., Calaycay, J., Mumford, R. A., Swiderek, K. M., Lee, T. D., and Nathan, C. (1992) Calmodulin is a subunit of nitric oxide synthase from macrophages, *J. Exp. Med. 176*, 599−604.
20. Aoyagi, M., Arvai, A. S., Tainer, J. A., and Getzoff, E. D. (2003) Structural basis for endothelial nitric oxide synthase binding to calmodulin, *EMBO J. 22*, 766−775.
21. Stevens-Truss, R., and Marletta, M. A. (1995) Interaction of Calmodulin with the Inducible Murine Macrophage Nitric Oxide Synthase, *Biochemistry 34*, 15638−15645.
22. Stevens-Truss, R., Beckingham, K., and Marletta, M. A. (1997) Calcium Binding Sites of Calmodulin and Electron Transfer by Neuronal Nitric Oxide Synthase, *Biochemistry 36*, 12337−12345.
23. Gao, Z. H., Krebs, J., VanBerkum, M. F. A., Tang, W.-J., Maune, J. F., Means, A. R., Stull, J. T., and Beckingham, K. (1993) Activation of Four Enzymes by two Series of Calmodulin Mutants with Point Mutations in Individual Ca^{2+} Binding Sites, *J. Biol. Chem. 268*, 20096−20104.
24. GuptaRoy, B., Beckingham, K., and Griffith, L. C. (1996) Functional Diversity of Alternatively Spliced Isoforms of *Drosophila* Ca^{2+}/Calmodulin-dependent Protein Kinase II: A role for the variable domain in activation, *J. Biol. Chem. 271*, 19846−19851.
25. Govers, R., and Rabelink, T. J. (2001) Cellular regulation of endothelial nitric oxide, *Am. J. Physiol. 280*, F193−F206.
26. Chen, P.-F., and Wu, K. K. (2000) Characterization of the Roles of the 594−645 Region in Human Endothelial Nitric-oxide Synthase in Regulating Calmodulin Binding and Electron Transfer, *J. Biol. Chem. 275*, 13155−13163.
27. Chen, P.-F., and Wu, K. K. (2003) Structural Elements Contribute to the Calcium/Calmodulin Dependence on Enzyme Activation in Human Endothelial Nitric-oxide Synthase, *J. Biol. Chem. 278*, 52392−52400.
28. Greif, D. M., Sacks, D. B., and Michel, T. (2004) Calmodulin phosphorylation and modulation of endothelial nitric oxide synthase catalysis, *Proc. Natl. Acad. Sci. U.S.A. 101*, 1165−1170.
29. Maune, J. F., Klee, C. B., and Beckingham, K. (1992) Ca^{2+} Binding and Conformational Changes in Two Series of Point Mutations to the Individual Ca^{2+}-binding Sites of Calmodulin, *J. Biol. Chem. 267*, 5286−5295.
30. Wu, C., Zhang, J., Abu-Soud, H., Ghosh, D. K., and Stuehr, D. J. (1996) High-Level Expression of Mouse Inducible Nitric Oxide Synthase in *Escherichia coli* Requires Coexpression with Calmodulin, *Biochem. Biophys. Res. Commun. 222*, 439−444.
31. Fossetta, J. D., Da Niu, X., Lunn, C. A., Zavodny, P. J., and Narula, S. K. (1996) Expression of human inducible nitric oxide synthase in *Escherichia coli*, *FEBS Lett. 379*, 135−138.
32. Rusche, K. M., Spiering, M. M., and Marletta, M. A. (1998) Reactions Catalyzed by Tetrahydrobiopterin-Free Nitric Oxide Synthase, *Biochemistry 37*, 15503−15512.
33. Perry, J. M., and Marletta, M. A. (1998) Effects of transition metals on nitric oxide synthase catalysis, *Proc. Natl. Acad. Sci. U.S.A. 95*, 11101−11106.
34. Hevel, J. M., and Marletta, M. A. (1994) Nitric-oxide synthase assays, in *Methods in Enzymololgy (Oxygen Radicals in Biological Systems. Part C)*, Vol. 233, pp 250−258, Academic Press, New York.
35. Alderton, W. K., Cooper, C. E., and Knowles, R. G., (2001) Nitric Oxide Synthases: Structure, function, and inhibition: A review Article, *Biochem. J. 357*, 593.
36. Hu, J., and Van Eldik, L. J. (1998) Regulation of Nitric Oxide Synthase by Calmodulin, in *Calmodulin and Signal Transduction* (Van Eldik, L. J., and Watterson, D. M., Eds.) pp 287−345, Academic Press, New York.
37. Lamas, S., Marsden, P. A., Li, G. K., Tempst, P., and Michel, T. (1992) Endothelial nitric oxide synthase: Molecular cloning and characterization of a distinct constitutive enzyme isoform, *Proc. Natl. Acad. Sci. U.S.A. 89*, 6348−6352.
38. Xie, Q.-W., Cho, H. J., Calaycay, J., Mumford, R. A., Swiderek, K. M., Lee, T. D., Ding, A., Troso, T., and Nathan, C. (1992) Cloning and characterization of inducible nitric oxide synthase from mouse macrophages, *Science 256*, 225−228.
39. Stuehr, D. J., Cho, H. J., Kwon, N. S., Weise, M. F., and Nathan, C. F. (1991) Purification and characterization of the cytokine-induced macrophage nitric oxide synthase: An FAD- and FMN-containing flavoprotein, *Proc. Natl. Acad. Sci. U.S.A. 88*, 7773−7777.
40. Schulz, D. M., Ihling, C., Clore, M., and Sinz, A. (2004) Mapping the Topology and Determination of a Low-Resolution Three-Dimensional Structure of the Calmodulin-Melittin Complex by Chemical Cross-Linking and High-Resolution FTICRMS: Direct Demonstration of Multiple Binding Modes, *Biochemistry 43*, 4703−4715.
41. Mukherjea, P., and Beckingham, K. (1993) Calcium Binding Site Mutants of Calmodulin Adopt Abnormal Conformations in

Complexes with Model Target Peptides, *Biochem. Mol. Biol. Int. 29*, 555−563.
42. Sorensen, B. R., Eppel, J. T., and Shea, M. A. (2001) Paramecium Calmodulin Mutants Defective in Ion Channel Regulation Associate with Melittin in the Absence of Calcium but Require It for Tertiary Collapse, *Biochemistry 40*, 896−903.
43. O'Neil, T. K., and Degrado, W. F. (1990) How calmodulin binds its targets: Sequence independent recognition of amphiphilic α-helices, *Trends Biochem. Sci. 15*, 59−64.
44. Kurokawa, H., Osawa, M., Kurihara, H., Katayama, N., Tokumitsu, H., Swindells, M. B., Kainosho, M., and Ikura, M. (2001) Target-induced Conformational Adaptation of Calmodulin Revealed by the Crystal Structure of a Complex with Nematode Ca^{2+}/Calmodulin-dependent Kinase Kinase Peptide, *J. Mol. Biol. 312*, 59−68.

BI0474517